Int. J. Heat Mass Transfer. Vol. 31, No. 1, pp. 67–77, 1988
Printed in Great Britain

0017–9310/88 $3.00 + 0.00

Local heat transfer coefficient in wavy free-falling turbulent liquid films undergoing uniform sensible heating

J. A. SHMERLER† and I. MUDAWWAR

Boiling and Two-phase Flow Laboratory, School of Mechanical Engineering, Purdue University, West Lafayette, IN 47907, U.S.A.

(*Received* 18 *March* 1987 *and in final form* 5 *June* 1987)

Abstract—Sensible heating of free-falling turbulent liquid films is investigated experimentally. The film flow exhibits rapid thermal development in the entrance region and enhanced heat transfer over the lower portion of the heated length. A correlation of an averaged fully developed heat transfer coefficient is presented as a function of Reynolds and Prandtl numbers. Measurements within the film showed the existence of a thermal boundary layer typical of turbulent channel flow. Numerical predictions of entrance and fully developed region heat transfer coefficients using established eddy diffusivity models are compared to the experimental data. The models predicted the extent of the development region but were not capable of predicting downstream enhancement of heat transfer since they do not account for wave activity at the film interface.

1. INTRODUCTION

PROPER evaluation of heat exchanger performance and cooling schemes for devices such as water-cooled turbine blades and computer chips requires the careful characterization of the transport mechanisms for thin liquid films. Previous analytical studies to determine heat transfer coefficients for hydrodynamically developed, sensibly heated films centered around the development of semi-empirical models for the eddy diffusivity terms that appear in the momentum and energy equations

$$\tau = \rho(\nu+\varepsilon_m)\frac{du}{dy} = \rho g(\delta - y) \tag{1}$$

$$u\frac{\partial T}{\partial x} = \frac{\partial}{\partial y}\left[\left(\alpha + \frac{\varepsilon_m}{Pr_t}\right)\frac{\partial T}{\partial y}\right]. \tag{2}$$

Early turbulence models used analogies to channel flow as was done by Seban [1] and Rohsenhow *et al.* [2] who used the universal velocity profile to solve equations (1) and (2). Dukler [3] used a two-part eddy diffusivity model using the Deissler equation near the wall and Von Karman's equation through the outer portion of the film. This model was later improved upon by Lee [4]. More recently, the Van Driest equation, which modifies the Von Karman linear mixing length equation with an exponential damping term to cause the eddy diffusivity term to go to zero at the wall, has been used to model turbulence in films [5–11]; however, the equation is only valid for the wall region, leaving the need for a model of turbulent activity at the film surface.

Modelling of turbulence in films is further complicated by wave activity at the film interface, which results in severe variation of local film thickness and continuous longitudinal changes in the hydrodynamic structure of falling films. Thus a hydrodynamically or thermally fully developed flow cannot be truly maintained in falling films.

Several approaches have been used to model the turbulent activity at the film interface. Gimbutis [5] and Mudawwar and El-Masri [6] used empirical functions to develop eddy diffusivity profiles that go to zero at the wall and also at the film interface. Mills and Chung [7], Seban and Faghri [8], and Hubbard *et al.* [9] used heat–mass transfer analogies with gas absorption experimental results to model turbulent activity at the film interface; however, the extent of the interface region has yet to be determined, leaving the validity of this approach questionable. Limberg [10] used the Van Driest equation up to $y^+ = 0.6\delta^+$ after which the eddy diffusivity was held constant over the rest of the film thickness. Yih and Liu [11] modified Limberg's model to take into account interfacial shear stress. In most cases, the turbulent Prandtl number was taken as 0.9 or 1.0, however, turbulent Prandtl number models have also been employed [6, 8, 9].

Although many approaches have been used to model momentum and heat transfer in falling films, assessment of the feasibility of any of these approaches requires a reliable data base for comparison with model predictions. Table 1 shows that the number of experimental studies has not been exhaustive. Investigations by Wilke [12], Ganchev *et al.* [13] and Gimbutis *et al.* [5, 14] resulted in correlations for the fully developed heat transfer coefficient as a function of Reynolds and Prandtl numbers. Fujita and Ueda's [15] data were too scattered

† Current address: AT&T Bell Laboratories, Liberty Corners, NJ 07060, U.S.A.

NOMENCLATURE

c_p	specific heat at constant pressure
g	acceleration due to gravity
h_H	heat transfer coefficient for sensible heating, $q_w/(T_w - T_m)$
h_H^*	dimensionless heat transfer coefficient, $(h_H v^{2/3})/(kg^{1/3})$
k	thermal conductivity
Ka	Kapitza number, $(\mu^4 g)/(\rho\sigma^3)$
L	length of the heated section
Pr	Prandtl number
Pr_t	turbulent Prandtl number, $\varepsilon_m/\varepsilon_h$
q	local heat flux
q_w	wall heat flux
Re	Reynolds number, $4\Gamma/\mu$
T	local temperature
T_{in}	inlet temperature
T_m	mean temperature
T_w	wall temperature
T^+	dimensionless temperature, $\rho c_p u^*(T_w - T)/q_w$
u	local velocity component in the flow direction
u^*	friction velocity, $\sqrt{(\tau_w/\rho)}$
u^+	dimensionless film velocity, u/u^*
x	longitudinal position from the entrance to the heated section
y	distance from the solid wall
y^+	dimensionless distance from the solid wall, yu^*/ν.

Greek symbols

α	thermal diffusivity
Γ	mass flow rate per unit film width
δ	film thickness
δ^+	dimensionless film thickness, $\delta u^*/\nu$
ε_h	eddy heat diffusivity
ε_m	eddy momentum diffusivity
μ	dynamic viscosity
ν	kinematic viscosity
ρ	liquid density
σ	surface tension
τ_w	wall shear stress.

to give any correlation and Oosthuzien and Cheung's [16] apparatus was not long enough to investigate fully developed conditions.

The present study reinvestigates sensible heating of falling films with an emphasis on high accuracy instrumentation to determine heat transfer coefficients over wide ranges of Reynolds and Prandtl numbers. An electrically heated thin walled stainless steel tube 781 mm long was used to determine the local heat transfer coefficient as a function of position along the heated length. Measurements were also made across the film thickness to determine the time-averaged temperature profile in turbulent falling films. Finally, a numerical study was performed using existing eddy diffusivity models to predict development region and fully developed heat transfer coefficients for comparison with the experimental results.

2. EXPERIMENTAL APPARATUS AND PROCEDURE

The test apparatus used in this study consisted of a closed loop high purity fluid delivery system which

Table 1. Experimental studies on sensible heating of falling films

	Authors					
	Wilke [12]	Ganchev *et al.* [13]	Gimbutis *et al.* [5, 14]	Fujita and Ueda [15]	Oosthuzien and Cheung [16]	Present study
Injection method	nozzle	nozzle	nozzle	sintered tube (70 mm)	brass nozzles	porous plastic tube (300 mm)
Tube diameter	42 mm o.d.	61.2 mm o.d.	30 mm o.d. 29 mm i.d.	16 mm o.d. 14 mm i.d.	25.4 and 19.1 mm o.d.	25.4 mm o.d. 24.6 mm i.d.
Adiabatic length	0	0	250 and 1580 mm	250 mm copper rod	0	757 mm G-10 plastic
Heated length	2400 mm	300 mm	500 and 1000 mm	600 and 1000 mm	370 mm	781 mm
Heating method	steam	hot water	electrical	electrical	electrical	electrical
Working fluid	water water/ethylene glycol	water	water	water	water	water
Reynolds number	8–10 000	~1620–13 600	1800–70 000	500–5000	20 000–70 000	2500–39 500
Prandtl number	5.4–210	2.74–10.6	4.3–8.4	2.2–6.6	5.1–5.6	2.5–6.87
Mean fluid temperature	measured	measured†	calculated	calculated	calculated	measured and calculated

† The local mean fluid temperature was assumed equal to that measured by a single thermocouple located in the film 0.1 mm away from the wall.

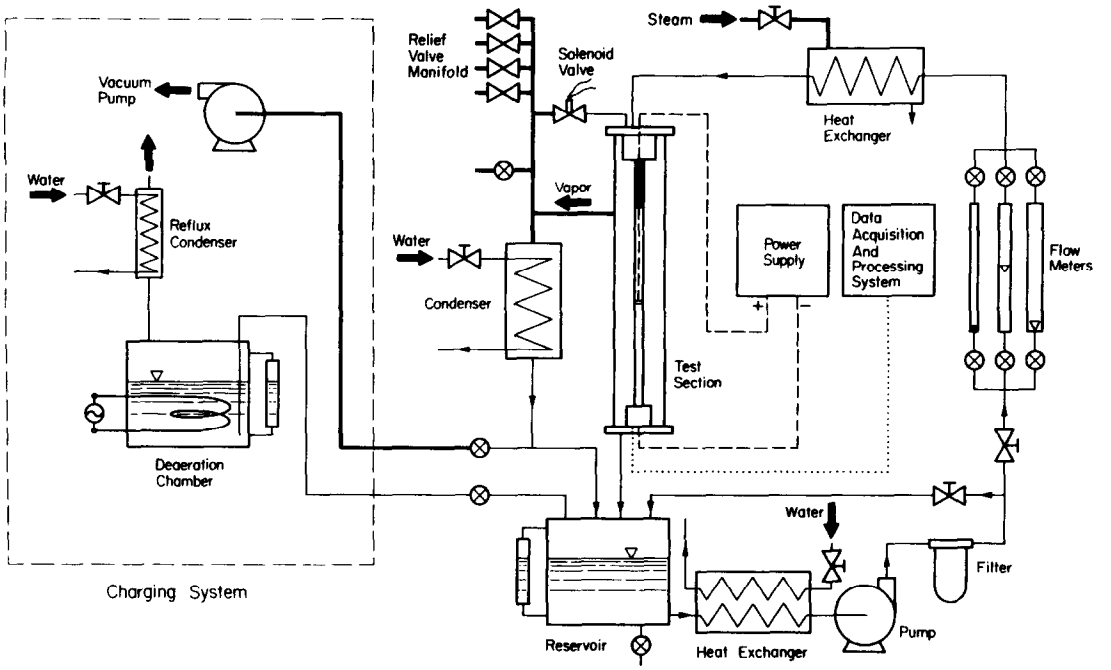

FIG. 1. Schematic diagram of the fluid delivery system.

supplied water over a 25.4 mm diameter, 1835 mm long test section. The test section was housed within a leak free chamber made of Lexgard, a polycarbonate plastic. The chamber consisted of two sections each having outer dimensions of $152.5 \times 152.5 \times 991$ mm and a wall thickness of 35 mm. A uniform film was created on the outside wall of the test section by feeding water from an upper reservoir into the center of a 300 mm long polyethylene tube having a mean porosity of 20 μm. The fluid was forced outward across the walls of the tube and driven by gravity over the rest of the test section. Following the porous distributor was a G-10 fiberglass plastic tube 757 mm long. This section allowed for development of the hydrodynamic boundary layer over an adiabatic boundary. A short coupling made of oxygen free copper was screwed into the bottom of the G-10 tube and soldered to the top of a stainless steel tube which served as the heated length. The stainless steel tube had a wall thickness of 0.41 mm, and length of 781 mm. Electrical connections were made to the coupling and to a copper lug soldered to the bottom of the heater tube. This allowed constant wall flux conditions to be simulated by passing a low voltage, high d.c. current (up to 15 V at 750 A) along the length of the stainless steel tube. Figure 1 shows a schematic of the experimental apparatus, and Fig. 2 shows a cross section of the test section and test chamber.

Heat transfer coefficients were determined by measuring the inside wall and mean film temperatures using copper–constantan thermocouples which were calibrated to an accuracy of 0.1°C. The wall temperature was measured at 17 locations by thermocouple pairs oriented 180° apart. Preliminary tests showed up to 50% difference between local heat transfer coefficients measured at diametrically opposite thermocouples due to misalignment of the test section. Thus the test section was designed to allow for thermal expansion and was carefully aligned before each test to ensure symmetrical film conditions. Each thermocouple was held in the head of a 6-32 nylon socket head cap screw by thermally conductive boron nitride epoxy as shown in Fig. 3. The epoxy covering the thermocouple bead was rounded to a profile identical to the inside of the heater tube. The threads closest to the screw head were removed leaving one to two threads at the bottom of the screw and a stainless steel spring was placed over the section without threads. The thermocouple screws were held by a Delrin tube machined to a close tolerance fit with the inside of the stainless steel tube. The screws were allowed to translate normal to the axis of the Delrin tube but were prevented from coming out of the tube by the few remaining threads. The screw heads were covered with a thermally conductive grease and pressed inward allowing the Delrin tube to be slid up inside the stainless steel tube. Once inside, the springs would force the screws outward ensuring that contact had been made with the heater wall.

The mean film temperature was determined with the aid of sampling scoops made of G-10 plastic as shown in Fig. 2. This technique was originally developed by Wilke [12] in his falling film studies. Measurements were made at four locations along the heated length with each location corresponding to an inside wall measurement position. Mean temperatures at the remaining positions were determined from an energy balance based on the measured values. The leading edges of the scoops were curved to match the

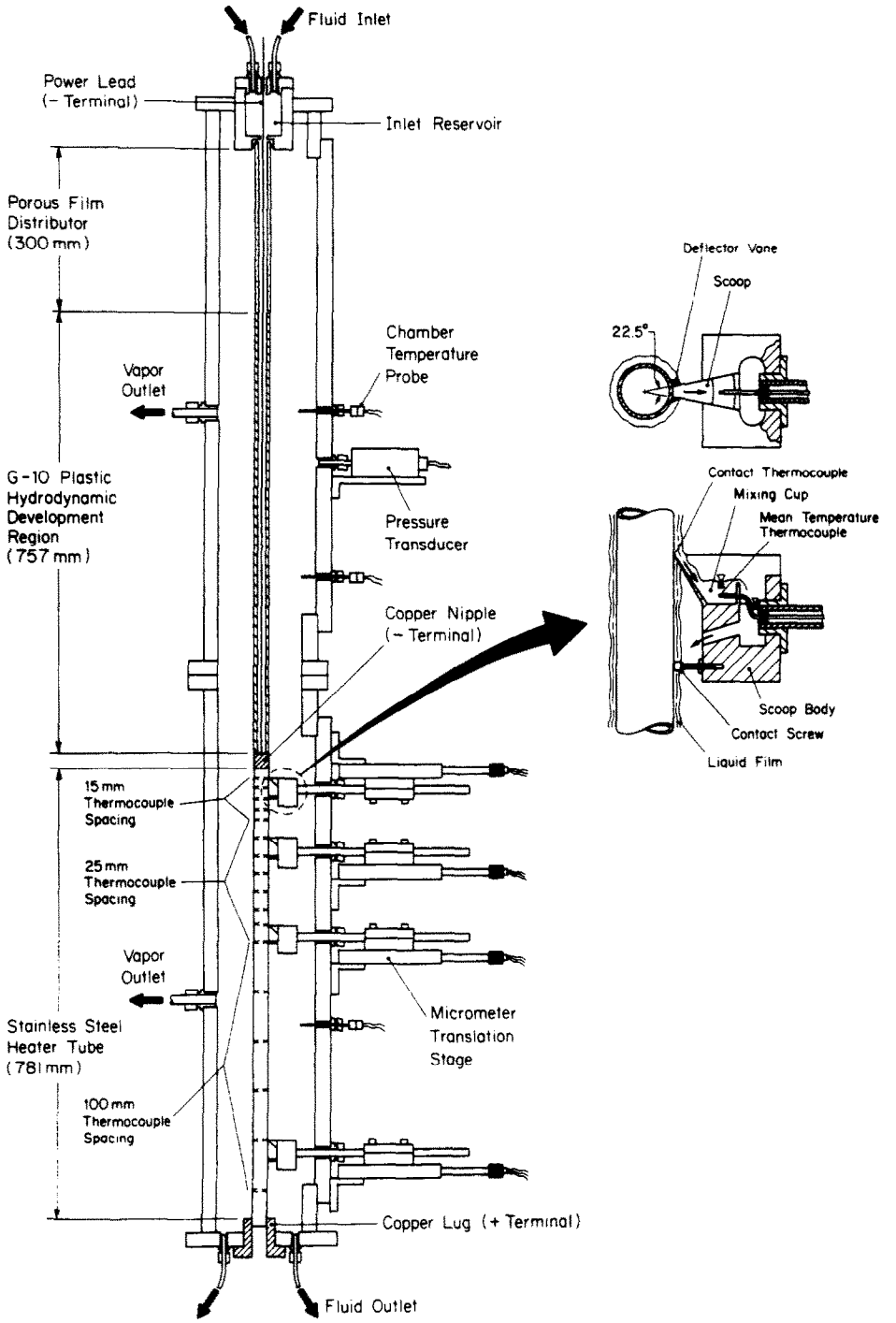

FIG. 2. Cut-away view of the test chamber.

outside radius of the stainless steel tube, and the walls of the scoop intersected the centerline of the heater tube at an angle of 22.5°, allowing the measured temperature to be in accord with the standard definition of a mean fluid temperature. When the scoop entered the film, the fluid would flow into a mixing cup in which a thermocouple bead was located. The liquid would then overflow the walls of the cup into the body of the scoop where it would be redeposited back onto the heated wall. To further insure that film dry-out would not occur, fins were placed below the scoop to cause a small portion of the film to be diverted to the area directly beneath the leading edge of the scoop. Contact with the heater wall was detected by a copper screw the head of which was aligned with the forward edge of the scoop. When the screw head touched the

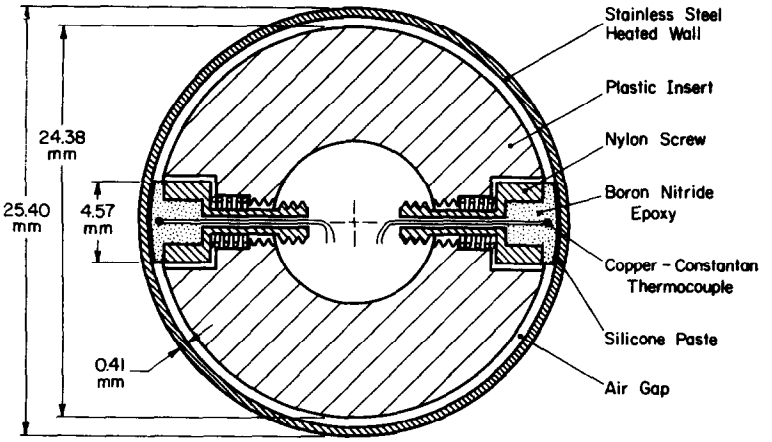

FIG. 3. Cross-sectional view of the inner thermocouple assembly.

heater wall, a secondary electric circuit would be formed, indicating that the scoop was in contact with the heater surface. One of the scoops was modified to determine the temperature profile by incorporating a small thermocouple bead into the leading edge of the scoop. A high accuracy micrometer translation stage was used for positioning each scoop within the film which allowed for local temperatures to be monitored.

Testing was performed using deionized water that was deaerated before introduction into the experimental apparatus as shown in Fig. 1. Once the system was charged, the fluid was circulated at the desired flow rate until a predetermined temperature was reached. The film inlet temperature was maintained through the control of the steam flow rate through the upstream heat exchanger. At this point, the power was turned onto the test section and increased to a level that gave a 5–10°C temperature rise across the film. The fluid was circulated under these conditions until the surrounding ambient reached a temperature close to the film temperature and atmospheric pressure and steady-state conditions within the film had been reached. The wall and system temperatures were recorded, and the sampling scoops were used one at a time proceeding from bottom to top along the test section to determine the mean film temperatures.

The mean film temperature was also calculated from an energy balance based on the measured temperature in the upstream sampling scoop, the measured wall temperature and the uniform heat flux supplied at the wall. Local mean temperature measurements were found to be within $\pm 10\%$ of the calculated values. Furthermore worse-case estimates of heat loss due to mass transfer by evaporation at the film interface were less than 7% of the total heat input.

3. EXPERIMENTAL RESULTS

Heat transfer results for films undergoing sensible heating have been obtained over a Reynolds number range of 2500 to 39 500 for Prandtl numbers between 2.55 and 6.87. Figures 4–7 are representative of the

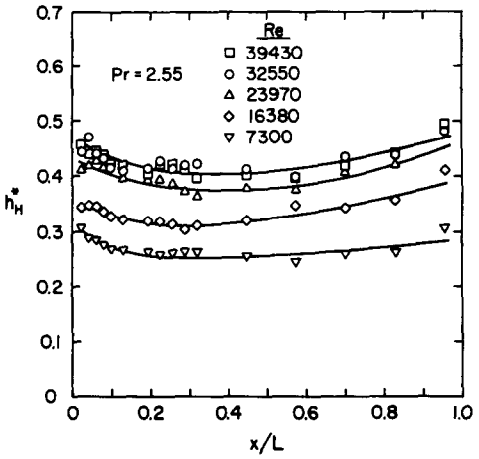

FIG. 4. Variation of the dimensionless heat transfer coefficient along the heated length for $Pr = 2.55$.

variation of the heat transfer coefficient as a function of dimensionless position, x/L, where L is the length of the heated test section. Fluid properties were based on the measured mean temperature to nondimensionalize the heat transfer coefficient, but for consistency between data sets, the reference Reynolds and Prandtl numbers indicated in Figs. 4–7 were determined from properties based on the fluid temperature in the inlet reservoir.

The flow was observed to exhibit rapid development of the thermal boundary layer as shown by the gradual decrease in h_H^* at the upstream measurement positions. The decrease in the heat transfer coefficient slowed near the middle of the heated length at which point h_H^* began a gradual increase rather than reaching a steady value as would be expected in turbulent channel flow.

Downstream heat transfer enhancement has been observed in previous falling film experiments. Ganchev *et al.* [13] performed experiments in which the instantaneous film thickness and local heat transfer coefficient were measured independently along a vertical test section. They developed empirical relation-

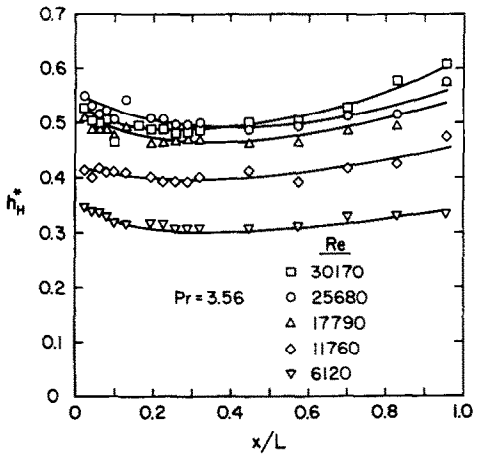

FIG. 5. Variation of the dimensionless heat transfer coefficient along the heated length for $Pr = 3.56$.

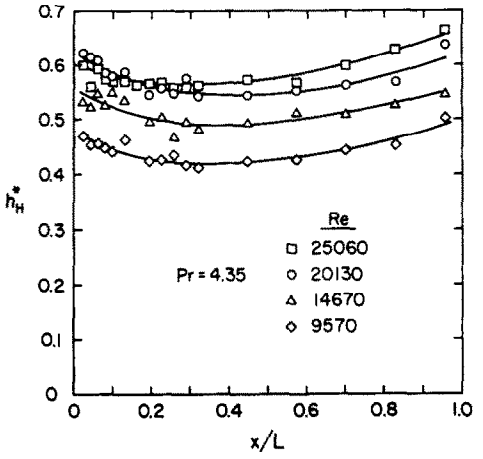

FIG. 6. Variation of the dimensionless heat transfer coefficient along the heated length for $Pr = 4.35$.

ships for calculating local values of the mean thickness and the heat transfer coefficient and demonstrated that changes in the nature of wave motion results in increases in the local heat transfer coefficient with film travel. Gimbutis [5] noted but did not specifically address this behavior, while Oosthuzien and Cheung [16] also attributed the enhancement to continuous changes in the hydrodynamic structure of falling films. This is a viable explanation of the phenomena and can be further substantiated by the results of the experiments performed by Takahama and Kato [17] and Salazar and Marschall [18] on surface waves in falling films. The study by Takahama and Kato showed that as the distance from the film inlet increased, the minimum film thickness decreased, eventually reaching an asymptotic value less than one half the mean film thickness. The maximum film thickness increased fairly linearly with distance as the film mass was accumulated into larger and faster turbulent waves. The growth of these large waves would result in an increase in the characteristic wavelength causing the time averaged film thickness to decrease with distance from the film inlet. This decrease was also

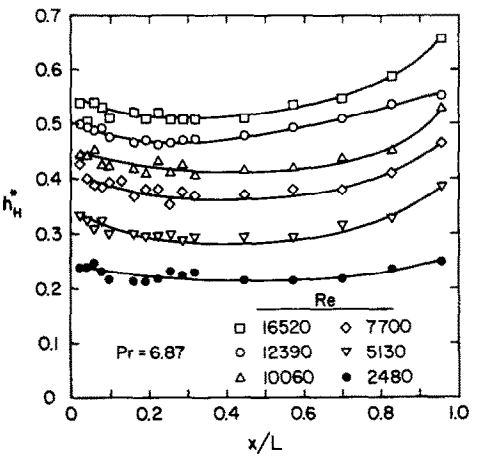

FIG. 7. Variation of the dimensionless heat transfer coefficient along the heated length for $Pr = 6.87$.

observed in the study by Salazar and Marschall. Thus, it can be speculated that the combination of a thinner film coupled with the increase in turbulent wave activity is the cause of the enhanced heat transfer over the lower portion of the heated length.

In addition to the wall and mean film temperatures, measurements were made within the film. The sampling scoop, instrumented with a small thermocouple bead at the leading edge, was positioned at fixed distances from the heated wall allowing for a qualitative assessment of the behavior of the temperature profile. When the temperature readings were unstable, the high and low temperatures were recorded. These values appear as boundaries for the curves shown in Figs. 8 and 9 which were obtained by the third sampling scoop. The scoop position within the film has been nondimensionalized with respect to the film thickness calculated from the correlation presented by Gimbutis [5] ($\delta_G = 0.136(\nu^2/g)^{1/3} Re^{0.583}$). The temperature was made dimensionless with respect to the measured wall and mean temperatures.

As shown in Figs. 8 and 9, the temperature exhibits a fairly logarithmic profile over the majority of operating conditions. As with the heat transfer enhancement observed over the lower portion of the heated length, the relationship between the temperature fluctuations and Reynolds number can be related to the hydrodynamic characteristics of the film. Although the thermal mass of the leading edge of the scoop might have damped the thermal response of the thermocouple to fluid temperature fluctuations, Figs. 8 and 9 provide a clear indication of the influence of flow conditions on these fluctuations. At low Reynolds numbers, waves moving past a fixed thermocouple would bring cooler fluid in contact with the thermocouple, causing significant temperature fluctuations. At higher Reynolds numbers the temperature decrease in the wall region takes place over a small fraction of the total film thickness leaving the bulk mixing to act on fluid at the same temperature. Therefore, the temperature fluctuations would be lim-

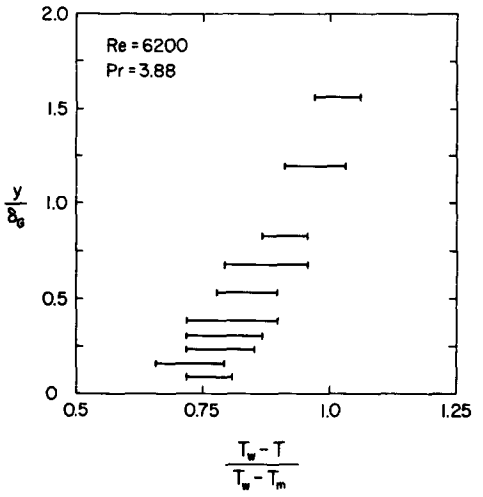

FIG. 8. Temperature variation with distance from the wall for $Re = 6200$ and $Pr = 3.88$.

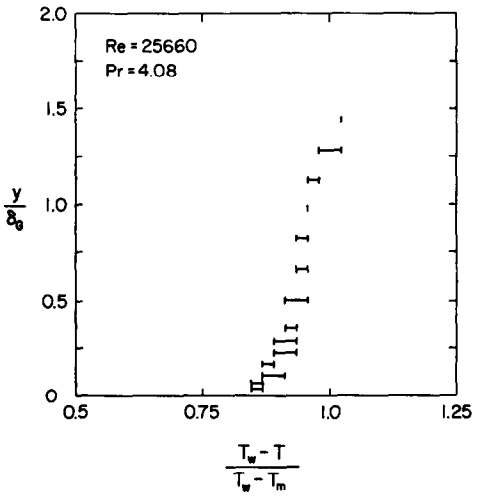

FIG. 9. Temperature variation with distance from the wall for $Re = 25\,660$ and $Pr = 4.08$.

ited to the wall region and would be less significant in the outer region where the temperature is fairly constant. These observations lead to the supposition that at high Reynolds numbers the effects of wave induced mixing may not be as pronounced as those caused by a thinner wall boundary layer.

Since the film interface is wavy, the value $\delta/\delta_G = 1$ in Figs. 8 and 9 corresponds to a mean reference thickness. The instantaneous thickness changes by as much as 250% above and 50% below the mean thickness δ_G [17]. Thus local temperature measurement at a distance δ_G away from the wall provides a transient signal which corresponds both to wave induced temperature fluctuations in the liquid and to temperature changes associated with the intermittence of the gas and liquid phases. Since the temperature probe could not be made to 'follow' the interface, the instantaneous interfacial temperature cannot be determined and its value can only be approximated using stationary probe measurements as shown in Figs. 8 and 9.

As shown by the data in Figs. 4–7, it would be unrealistic to determine a correlation for a fully developed heat transfer coefficient, since asymptotic behavior was never observed. However, a correlation was determined for an average heat transfer coefficient as a function of local Reynolds and Prandtl numbers based on measured values of T_m. An average value for h_H^* was found by determining the mean value from the longitudinal position where the minimum value occurred to the next to last measurement position. The last position was excluded because it was felt that liquid splashing might have affected the temperature measurements in that location. The average heat transfer coefficient was correlated as

$$h_H^* = 0.0106 Re^{0.3} Pr^{0.63}. \quad (3)$$

The correlation, Fig. 10, has an average error of 5.5% with a maximum error and standard deviation of 17% and 0.031, respectively. This correlation predicts the fully developed data presented by Oosthuzien and Cheung [16] for $Re = 24\,850$ and $Pr = 5.54$ with an accuracy of 2.0%.

For Reynolds numbers below 5000, the correlation was compared to the data of Fujita and Ueda [15], and to the correlation given by Wilke [12]. It should be noted that the data of Fujita and Ueda are only those values taken at power levels 30–70% of the heat flux necessary to cause film breakdown. As shown in Fig. 11, the present correlation predicts values higher than the data of Fujita and Ueda, but the large amount of scatter makes it difficult to quantify the difference between the two studies. With respect to Wilke's correlation, there was fair agreement at the highest Prandtl number. The disagreement at the lower Prandtl number can be attributed to the flow conditions being outside of Wilke's experimental range; the lowest Prandtl number achieved in his study was 5.4. Furthermore, there were differences in the methods of introducing the film and wall boundary condition. Wilke used a nozzle to form his film, and a steam jacket to simulate isothermal rather than constant wall heat flux conditions.

At Reynolds numbers greater than 5000, a comparison of the present correlation was made to the correlation presented by Gimbutis [5]. This comparison is shown in Fig. 12 for a Prandtl number of 3.55. As shown, the present correlation predicts values approximately 25% lower than those determined using Gimbutis' correlation. This disagreement may be attributed in part to the relatively high Prandtl number range associated with Gimbutis' correlation. Again, there was a difference in the method of fluid injection which might have resulted in hydrodynamic differences between the two studies. It should also be noted that Gimbutis did not measure the mean film temperature, but relied on an energy balance based on the inlet reservoir and outlet temperature to interpolate mean temperatures at various longitudinal positions. This method was found to be inaccurate since the adiabatic entrance section was not necessarily iso-

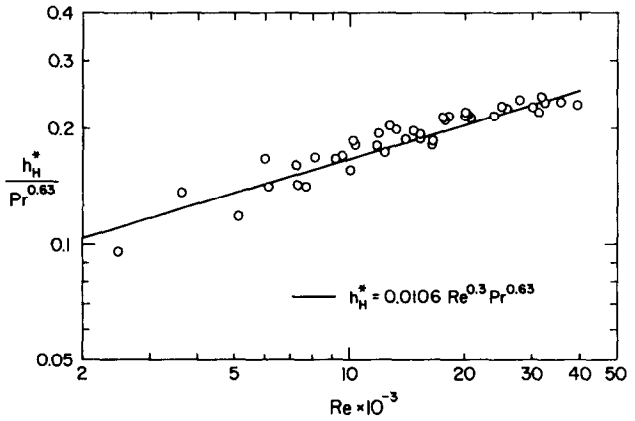

FIG. 10. Correlation of the dimensionless heat transfer coefficient for $Re = 2480$–$39\,430$ and $Pr = 2.55$–6.87.

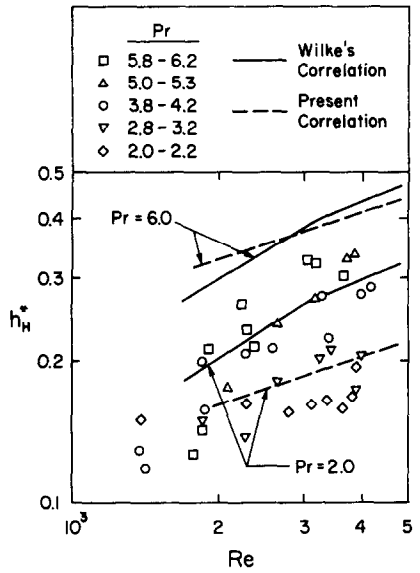

FIG. 11. Comparison of the present correlation to the correlation of Wilke [12] and the data of Fujita and Ueda [15].

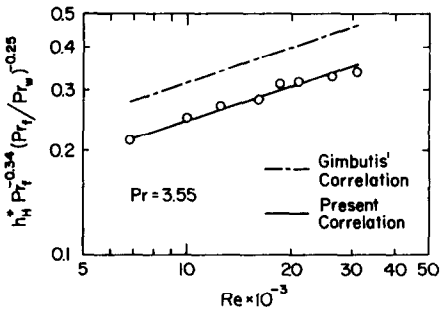

FIG. 12. Comparison of experimental data to Gimbutis' correlation [5] for $Pr = 3.55$.

thermal. In the present study, temperature reductions of up to 1.5°C were detected from the inlet reservoir to the start of the heated test section. Not accounting for this temperature decrease would result in the prediction of higher mean temperatures and consequently higher heat transfer coefficients.

The study by Ganchev *et al.* [13] provided important findings concerning the relationship between longitudinal changes in film waviness and heat transfer with film travel. Since they used hot water to heat the working fluid, the wall heat flux had to be determined with a relatively high degree of uncertainty from temperature measurements in both fluids. Furthermore, Ganchev *et al.* did not sample the film to measure its mean temperature. Instead, the local mean fluid temperature T_m was assumed equal to that measured by a single thermocouple located within the film 0.1 mm away from the wall. As shown in Fig. 8 this technique leads to serious errors (up to 50% of the measured value) since a distance of 0.1 mm corresponds to a position within the laminar sublayer especially for the relatively low Reynolds number range ($1620 \lesssim Re \lesssim 13\,600$) associated with Ganchev *et al.*'s study.

Other factors which may have contributed to differences between the present correlation and those of other investigators include misalignment and/or buckling of the test section due to thermal expansion. As mentioned in Section 2, these problems may cause significant errors in mean temperature measurement due to the loss of circumferential symmetry of film flow.

4. NUMERICAL RESULTS

A closed form solution of the momentum and energy equations is hindered by the appearance of the turbulence terms in equations (1) and (2). However, heat transfer coefficients can be determined numerically using semi-empirical eddy diffusivity models. Two different techniques are used in the present study to determine the fully developed and development region heat transfer coefficient.

To predict fully developed heat transfer coefficients, a numerical integration of equation (2) was performed assuming $\partial T/\partial x = dT_m/dx$ to determine the dimensionless mean temperature. As shown in refs. [6, 19]

$$T_m^+ = \int_0^{\delta^+} \frac{\left[1 - \int_0^{y^+} \frac{u^+ \, dy^+}{Re/4}\right]^2}{\frac{1}{Pr} + \frac{1}{Pr_t}\frac{\varepsilon_m}{\nu}} dy^+ \quad (4)$$

where

$$u^+ = \int_0^{y^+} \frac{1 - \frac{y^+}{\delta^+}}{1 + \frac{\varepsilon_m}{\nu}} dy^+ \quad (5a)$$

$$Re = 4 \int_0^{\delta^+} u^+ \, dy^+. \quad (5b)$$

The integrals were evaluated using Gauss–Legendre quadratures with sixth-degree Legendre polynomials. From the solution for T_m^+, fully developed heat transfer coefficients could then be determined

$$h_H^* = \frac{(\delta^+)^{1/3} Pr}{T_m^+}. \quad (6)$$

The second method used the finite difference technique with a marching solution along the heated length. The model assumes a constant film thickness, a fully developed velocity profile (from a numerical integration of equation (5a)), and negligible curvature effects. The governing energy equation was reduced to equation (2), assuming that only radial conduction and longitudinal advection occurred. The boundary conditions for a sensibly heated film take the following form:

$$x = 0 \quad T = T_{in}$$

$$y = 0 \quad \frac{\partial T}{\partial y} = \frac{-q_w}{k}$$

$$y = \delta \quad \frac{\partial T}{\partial y} = 0.$$

The energy equation was discretized over an equally spaced grid and solved at each axial location using the Thomas algorithm. Once the temperature at each node was determined, the mean temperature was found through an integration using Simpson's 1/3 rule. For both numerical techniques, the eddy diffusivity functions of Limberg [10], Hubbard *et al.* [9] and Mudawwar and El-Masri [6], Table 2, were used in evaluating the eddy diffusivity term and the turbulent Prandtl number was taken equal to 0.9.

Figure 13 shows the results for h_H^* as a function of longitudinal position along the heated length as determined from the finite difference solution at a

Table 2. Turbulence models of free-falling films used for comparison with experimental data

Author	Range	Eddy diffusivity
Limberg [10]	$0 \leqslant y^+ < 0.6\delta^+$	$\frac{\varepsilon_m}{\nu} = \frac{-1}{2} + \frac{1}{2} \times \sqrt{\left(1 + 4K^2 y^{+2}\left[1 - \exp\left\{\frac{-y^+\left(1 - \frac{y^+}{\delta^+}\right)^{1/2}}{A^+}\right\}\right]^2 \left(1 - \frac{y^+}{\delta^+}\right)\exp\left(-3.32\frac{y^+}{\delta^+}\right)\right)}$
	$0.6\delta^+ \leqslant y^+ \leqslant \delta^+$	$\frac{\varepsilon_m}{\nu} = \left.\frac{\varepsilon_m}{\nu}\right\|_{y^+ = 0.6\delta^+}$ $K = 0.41$; $A^+ = 25.1$
Hubbard *et al.* [9]	$0 \leqslant y^+ < y_i^+$	$\frac{\varepsilon_m}{\nu} = \frac{1}{2} + \frac{1}{2}\sqrt{\left(1 + 4K^2 y^{+2}\left[1 - \exp\left(-\frac{y^+}{A^+}\right)\right]^2 \left(1 - \frac{y^+}{\delta^+}\right)\right)}$
	$y_i^+ \leqslant y^+ \leqslant \delta^+$	$\frac{\varepsilon_m}{\nu} = \frac{8.13 \times 10^{-17}}{Ka} \cdot \frac{Re^{2m}}{\delta^{+2/3}} (\delta^+ - y^+)^2$ $K = 0.4$; $A^+ = 26$; $m = 6.95 \times 10^2 \nu^{1/2}$, ν in $m^2\,s^{-1}$
Mudawwar and El-Masri [6]	$0 \leqslant y^+ \leqslant \delta^+$	$\frac{\varepsilon_m}{\nu} = -\frac{1}{2} + \frac{1}{2} \times \sqrt{\left(1 + 4K^2 y^{+2}\left(1 - \frac{y^+}{\delta^+}\right)^2 \left[1 - \exp\left\{-\frac{y^+}{26}\left(1 - \frac{y^+}{\delta^+}\right)^{1/2}\left(1 - \frac{0.865 Re_{crit}^{1/2}}{\delta^+}\right)\right\}\right]^2\right)}$ $Re_{crit} = \frac{97}{Ka^{0.1}}$ $K = 0.40$; $A^+ = 26$

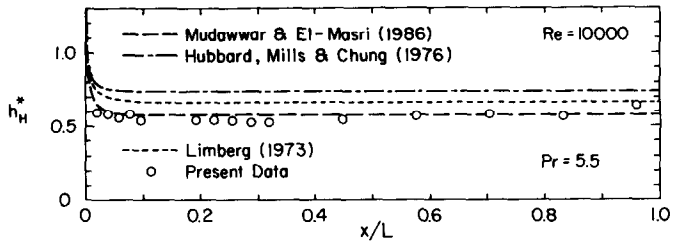

FIG. 13. Comparison of experimental data and numerical predictions of the local heat transfer coefficient for $Pr = 5.5$.

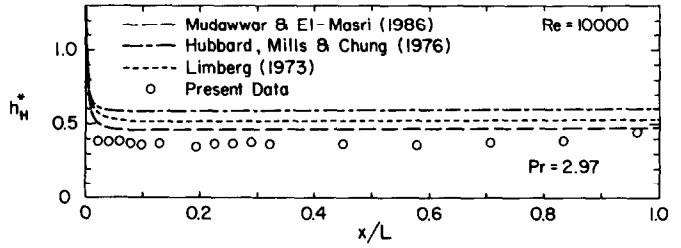

FIG. 14. Comparison of experimental data and numerical predictions of the local heat transfer coefficient for $Pr = 2.97$.

Reynolds number of 10 000 and a Prandtl number of 5.5. The asymptotic values at the outlet of the heated section predicted using this method were within 2% of the values determined by the integral solution of equation (4) for fully developed values. The model presented by Mudawwar and El-Masri was closest to predicting the data. All three models were in fair agreement with the shape and extent of the development length exhibited by the data, but failed to predict the trend of increasing h_H^* over the lower portion of the heated length. A similar behavior can be seen in Fig. 14, although there was a greater overprediction of the data at the lower Prandtl number. Failure of the models to predict downstream enhancement of heat transfer was to be expected since they all assume a smooth film and do not take into direct account the effect of surface waves.

For both Prandtl number cases, the model of Hubbard *et al.* overpredicted the data. This can be attributed to several factors. Hubbard *et al.*'s model was originally developed to predict evaporation data, and was not verified for use with films subjected to uniform sensible heating. Also, the mass transfer analogy used to model the turbulent activity at the interface has never been justified experimentally. The extent of the interface region has been arbitrarily extended to the intersection with the Van Driest function which applies for the wall region. Furthermore, it is not certain whether an empirical eddy diffusivity profile obtained from large Schmidt number mass transfer experiments is valid for low Prandtl number heat transfer experiments.

5. CONCLUSIONS

The experimental results for sensible heating of a turbulent free-falling film have been presented. A short development length and enhancement over the lower portion of the heated length were characteristic of the flow. The enhanced heat transfer was attributed to the changing hydrodynamic characteristics of the flow with longitudinal position. Local temperature measurements within the film showed the presence of a turbulent boundary layer profile and decreased temperature fluctuations with an increase in the Reynolds number. A correlation for the averaged heat transfer coefficient was found as a function of Reynolds and Prandtl numbers.

Numerical studies were performed using existing eddy diffusivity models to predict heat transfer coefficients in the development and the fully developed regions. The models predicted the extent of the development region but were not very accurate in predicting fully developed values for h_H^* and the enhanced heat transfer. It is felt that future models should incorporate characteristic wave information to more realistically model falling films.

Acknowledgement—This study was supported by a research grant from the U.S. Department of Energy, Office of Basic Sciences (Grant No. DE-FGO2-85ER13398), and a faculty assistance grant from Amoco Oil Company.

REFERENCES

1. R. A. Seban, Remarks on film condensation with turbulent flow, *Trans. ASME* **76,** 299–303 (1954).
2. W. M. Rohsenhow, J. H. Webber and A. T. Ling, Effect of vapor velocity on laminar and turbulent film condensation, *Trans. ASME* **78,** 1637–1643 (1956).
3. A. E. Dukler, Fluid mechanics and heat transfer in vertical falling-film systems, *Chem. Engng Prog.* **56,** 1–10 (1960).
4. J. Lee, Turbulent film condensation, *A.I.Ch.E. Jl* **10,** 540–544 (1964).

5. G. Gimbutis, Heat transfer of a turbulent falling film, *Proc. 5th Int. Heat Transfer Conf.*, Tokyo, Japan, Vol. 2, pp. 85–89 (1974).
6. I. A. Mudawwar and M. A. El-Masri, Momentum and heat transfer across freely-falling turbulent liquid films, *Int. J. Multiphase Flow* **12,** 771–790 (1986).
7. A. F. Mills and D. K. Chung, Heat transfer across turbulent falling films, *Int. J. Heat Mass Transfer* **16,** 694–697 (1973).
8. R. A. Seban and A. Faghri, Evaporation and heating with turbulent falling liquid films, *J. Heat Transfer* **98,** 315–318 (1976).
9. G. L. Hubbard, A. F. Mills and D. K. Chung, Heat transfer across a turbulent falling film with concurrent vapor flow, *J. Heat Transfer* **98,** 319–320 (1976).
10. H. Limberg, Warmeubergang an turbulente und laminare rieselfilme, *Int. J. Heat Mass Transfer* **16,** 1691–1702 (1973).
11. S. M. Yih and J. L. Liu, Prediction of heat transfer in turbulent falling films with or without interfacial shear, *A.I.Ch.E. Jl* **29,** 903–909 (1983).
12. W. Wilke, Warmeubergang an rieselfilme, *VDI ForschHft. 490* (1962).
13. B. G. Ganchev, V. M. Koglov and V. V. Lozovetskiy, A study of heat transfer to a falling fluid film at a vertical surface, *Heat Transfer—Soviet Res.* **4,** 102–110 (1972).
14. G. J. Gimbutis, A. J. Drobacivius and S. S. Sinkunas, Heat transfer of a turbulent water film at different initial flow conditions and high temperature gradients, *Proc. 6th Int. Heat Transfer Conf.*, Toronto, Canada, Vol. 1, pp. 321–326 (1978).
15. T. Fujita and T. Ueda, Heat transfer to falling liquid films and film breakdown—I, *Int. J. Heat Mass Transfer* **21,** 97–108 (1976).
16. P. H. Oosthuzien and T. Cheung, An experimental study of heat transfer to developing water film flow over cylinders, *J. Heat Transfer* **99,** 152–155 (1977).
17. H. Takahama and S. Kato, Longitudinal flow characteristics of vertically falling liquid films without concurrent gas flow, *Int. J. Multiphase Flow* **6,** 203–215 (1980).
18. R. P. Salazar and E. Marschall, Time-averaged local thickness measurements in falling liquid film flow, *Int. J. Multiphase Flow* **4,** 405–412 (1978).
19. J. A. Shmerler, A study of sensible heating and evaporation in free-falling liquid films, MSME thesis, Purdue University, West Lafayette, Indiana (1986).

COEFFICIENT DE TRANSFERT THERMIQUE LOCAL DANS DES FILMS TOMBANTS LIQUIDES, TURBULENTS, AVEC CHAUFFAGE SENSIBLE UNIFORME

Résumé—Le chauffage sensible de films tombants, liquides, turbulents est étudié expérimentalement. L'écoulement subit un rapide développement thermique dans la région d'entrée et augmente le transfert thermique sur la portion inférieure de la longueur chauffée. Une formule pour le coefficient de transfert moyen pleinement développé le présente en fonction des nombres de Reynolds et de Prandtl. Des mesures dans le film montrent l'existence d'une couche limite thermique typique de l'écoulement turbulent en canal. Des prédictions numériques des coefficients de transfert thermique dans les régions d'entrée et pleinement établi, utilisant des modèles de diffusivité thermique, sont comparées aux données expérimentales. Les modèles prédisent l'étendue de la région de développement mais ils ne sont pas capables de prédire l'accroissement du transfert en aval, car ils ne prennent pas en compte l'activité des ondes à l'interface du film.

ÖRTLICHE WÄRMEÜBERGANGS-KOEFFIZIENTEN IN WELLIGEN, FREI FALLENDEN, TURBULENTEN FLÜSSIGKEITSFILMEN BEI SENSIBLER AUFHEIZUNG

Zusammenfassung—Die sensible Aufheizung von freifallenden, turbulenten Flüssigkeitsfilmen wurde experimentell untersucht. Die Filmströmung zeigt eine schnelle thermische Entwicklung im Einlaufbereich und einen erhöhten Wärmeübergang im unteren Teil der beheizten Länge. Es wird eine Beziehung für den Wärmeübergangskoeffizienten der voll entwickelten Filmströmung in Abhängigkeit von Reynolds- und Prandtl-Zahl angegeben. Messungen im Film zeigten die Existenz einer Wärmegrenzschicht, wie sie für turbulente Kanalströmungen typisch ist. Berechnungen der Wärmeübergangskoeffizienten im Eintritts- und im voll entwickelten Bereich, die auf bewährte Modelle mit turbulenten Transportgrößen zurückgreifen, wurden mit den experimentellen Daten verglichen. Die Modelle sagten die Ausmaße des Einlaufbereichs voraus, waren aber nicht fähig, die Erhöhung des Wärmeübergangs stromab vorauszusagen, weil sie die Wellenbildung an der Filmoberfläche nicht berücksichtigen.

ЛОКАЛЬНЫЙ КОЭФФИЦИЕНТ ТЕПЛООБМЕНА В ВОЛНООБРАЗНЫХ СВОБОДНО СТЕКАЮЩИХ ТУРБУЛЕНТНЫХ ПЛЕНКАХ ЖИДКОСТИ ПРИ РАВНОМЕРНОМ НАГРЕВЕ

Аннотация—Экспериментально исследовался нагрев свободно стекающих турбулентных пленок жидкости. Пленка характеризуется быстропротекающими тепловыми процессами в начальной части и более интенсивным теплопереносом в нижней части участка нагрева. Получена зависимость осредненного коэффициента теплопереноса в полностью развитом участке от чисел Рейнольдса и Прандтля. Измерениями, проведенными непосредственно в пленке, обнаружено существование теплового пограничного слоя, характерного для турбулентного течения в канале. Результаты численных расчетов коэффициентов теплообмена на начальном участке и в зоне полностью развитого теплообмена с помощью известных моделей турбулентной температуропроводности сравниваются с экспериментальными данными. Эти модели позволяют рассчитать протяженность начальной зоны, но оказались непригодными для описания интенсификации теплообмена вниз по течению, так как не учитывают волновой характер поверхности пленки.